10.1127/s11727-013-1165-z

Front. Earth Sci.

Ci SONG et al. Sensitivity studies of methane column concentration inversion

RESEARCH ARTICLE

Sensitivity studies of high-precision methane column concentration inversion using a line-by-line radiative transfer model

Ci SONG[1], Jiong SHU[1](✉), Mandi ZHOU[1], Wei GAO[1,2]

1. Key Lab. of Geographic Information Science, East China Normal Shanghai 200241, China
2. Department of Ecosystem Science and Sustainability and Natural Resource Ecology Laboratory , Colorado State University, Colorado, 80523, US

Abstract. Hyper-spectral remote sensing may provide an effective solution to retrieve the methane (CH_4) concentration in an atmospheric column. As a result of exploring the absorptive characteristics of CH_4, an appropriate band is selected from the hyperspectral data for the detection of its column concentration with high precision. Following the most recent inversion theory and methods, the line-by-line radiative transfer model (LBLRTM) is employed to forward model the impact of four sensitive factors on inversion precision, including CH_4 initial profile, temperature, overlapping gases, and surface albedo. The study results indicate that the four optimized factors could improve the inversion precision of atmospheric CH_4 column concentration.

Keywords: methane, inversion, radiance, sensitivity, forward model, high precision.

1 Introduction

Methane (CH_4) is the most abundant hydrocarbon in the atmosphere; it is also one of the most important atmospheric greenhouse gases (CO2, CH4, NO2, O3, HFCs, PFCs, SF6) Kyoto (1998), affected by human activities. Because of the increased burden of CH_4 in the atmosphere, its contribution to radiance forcing is 0.48w/m^2 , which is approximately 18% of the overall radiative forcing by long-lived greenhouse gases (LLGHGs) (Khalil M A K and Rasmussen R A, 1984), making CH4 the second most important LLGHGs. Approximately 40% of the CH_4 emitted into the atmosphere comes from natural sources, such as wetlands and termites, whereas anthropogenic sources, such as ruminants, rice agriculture, fossil fuel exploitation, landfills, and biomass burning, account for approximately 60%. The globally averaged CH_4 concentration in 2010 was 1.808 ppmv, an increase of 0.28% compared with 2009, and 258% compared with 1750 (Barrie L A et al., 2011). Although the CH4 concentration in the atmosphere is far less than that of carbon dioxide (CO2), its greenhouse effect by unit concentration is 25 times larger than that of CO2(Forster P, 2007). The continual growth of the atmospheric CH_4 concentration effects the Earth's radiation balance and thus directly influences climate change (Parker R, 2011).

CH_4 is also an important chemical in terms of active carbon composition. Its chemical effect in the troposphere affects the concentrations of hydroxyl radicals (OH) and carbon monoxide (CO)

(Etheridge D et al., 1992; Grutzen P J, 1995). The chemistry of CH_4 plays an important role in determining the chemical composition of the atmosphere and indirectly affects climate and the environment, which in turn affect human survival. Approximately 85% of CH_4 molecules emitted to the atmosphere are removed by oxidation (Bergamaschi P et al., 2005; Frankenberg C et al., 2011). This process is initiated by reaction with the hydroxyl radical (OH) (Dlugokencky E J et al., 1994; Qin Y and Zhao C S, 2003):

$$CH4 + OH \rightarrow CH3 + H2O$$
$$CH3 + O2 + M \rightarrow CH3O2 + M$$
$$CH3O2 + 3O2 + M \rightarrow CH2O + OH + 2O3$$
$$CH2O + 4O2 + 2h\nu \rightarrow CO + 2OH + 2O3$$
$$CO + 2O2 + h\nu \rightarrow CO2 + O3$$

CH_4 oxidation eventually produces CO2 and may also yield ozone (O3) under conditions where the nitric oxide mixing ratio exceeds 5 to 10 ppt (parts per trillion, where 1 trillion = 10^{12}, by volume) (Dlugokencky E J et al., 1994). The impacts of CH_4 on climate change probably go beyond the previous estimates.

However, the research on CH_4 is lacking. Intermittent, scattered observations of CH4 date back to the 1960s, whereas systematic research on CH_4 began in the 1980s (Zhou L X and Li J L, 1990). To further study CH_4 sources, sinks, and variation, scientists have been vigorously developing satellite remote sensing monitoring over the past 10 years. This technique can provide stable, long-term atmospheric CH4 information on a global scale and with good space-time consistency, thus effectively compensating for the deficiency in near-surface observations.

The observation data indicate that global warming is closely related to increasing greenhouse gas emissions over the past 100 years. However, the correlation between greenhouse gases and global warming is still not clear due to a lack of understanding of greenhouse gas sources and sinks. As a first procedure to solve the above problem, the realization of high-precision detection of global CH_4 is crucial for assessing future global warming trends. Making full use of the high sensitivity and resolution data will help to improve the inversion precision of CH_4 column concentration by considering all factors such as initial profile, temperature, interference of overlapping gas absorption, and surface albedo.

Several fundamental papers using different techniques have recently researched the sensitivity studies of CO_2. J. P. Mao and S. R. Kawa (2003) have discussed the sensitivity Studies for spacebased measurement of atmospheric total column carbon dioxide by reflected sunlight. Tie Dai and Guangyu Shi (2008) have shown the numerical simulation study of atmospheric CO_2 concentration from FY-3 satellite. Hanhan Ye et al. (2011) have displayed the sensitivity for retrieval of atmospheric column carbon dioxide with high accuracy. However, few work was reported on the sensitivity of atmospheric CH_4 retrieval in both theoretical and applied research.

In this paper, the basic absorptive features of the 7.66μm band for a realistic atmosphere with absorption are first described. The dependence of the radiance sensitivity on the CH_4 initial profile, temperature, overlapping gases, and surface albedo data are also addressed. This study focuses on the response of the back-to-space radiances in the 7.66μm band to the boundary layer atmospheric CH4 change in relation to the response to other variables. The previous studies are extended through examining the spectral sensitivity of the detected radiances over a varied set of atmospheric conditions in greater detail using the line-by-line radiative transfer model (LBLRTM)

(http://rtweb.aer.com/lblrtm.html). The pivotal problem is how to try out the impact of four sensitive factors, including CH_4 initial profile, temperature, overlapping gases, and surface albedo, on inversion precision. Although specific instrumentation or instrument characteristics are not included, the results of this study may provide a potential solution for the development of future forward models and a precise inversion algorithm.

2 CH_4 Absorption

2.1 Absorption Characteristics of Atmospheric Molecules

Solar radiation is absorbed, reflected, refracted, and scattered when passing through the atmosphere. The attenuation extent differs by electromagnetic wave bands. Atmospheric absorption refers to the radiation which is reflected back into space when sunlight passes through the atmosphere to the ground. Atmospheric molecules have many infrared absorption bands. The sunlight carries information about the abundance of atmospheric molecules when it passes through the atmosphere, from which it can be obtained information about the total absorbing gas content and the vertical distribution. The solar radiation absorption of H2O, CO2, and O3 are the most significant of all the atmospheric gases.

2.2 Absorption Spectrum

Generally, to achieve signal detection with a high signal-to-noise ratio, the band for the inversion of gas concentration should have strong radiative intensity. However, in this band, the strength of gas absorption should be moderate: if it is too weak, it will not be sensitive to concentration change; if it is too strong, it will easily saturate the detector. In this study, the band of 1200–1400 cm^{-1} is choosed from the HITRAN (high-resolution transmission molecular absorption) 2008 database Rothman L S et al. (2009) to invert. In the atmosphere, the approximate total vertical column contents are as follows: CH4, 3.4×10^{19} molecules/cm2; H2O, 4.6×10^{22} molecules/cm2; O3, 6.8×10^{18} molecules/cm^2; N2O, 6.0×10^{18} molecules/cm2; CO, 1.8×10^{18} molecules/cm^2 (Shi G Y, 2007). Considering the content of these gas molecules in the atmosphere, the LBLRTM is used to model the atmospheric transmissivity assuming that each of the above gas molecules exists alone (atmospheric conditions using the U.S. standard atmosphere). As shown in Fig.1, the main interferences for CH4 inversion are H2O and N2O in the band of 1200–1400 cm^{-1}.

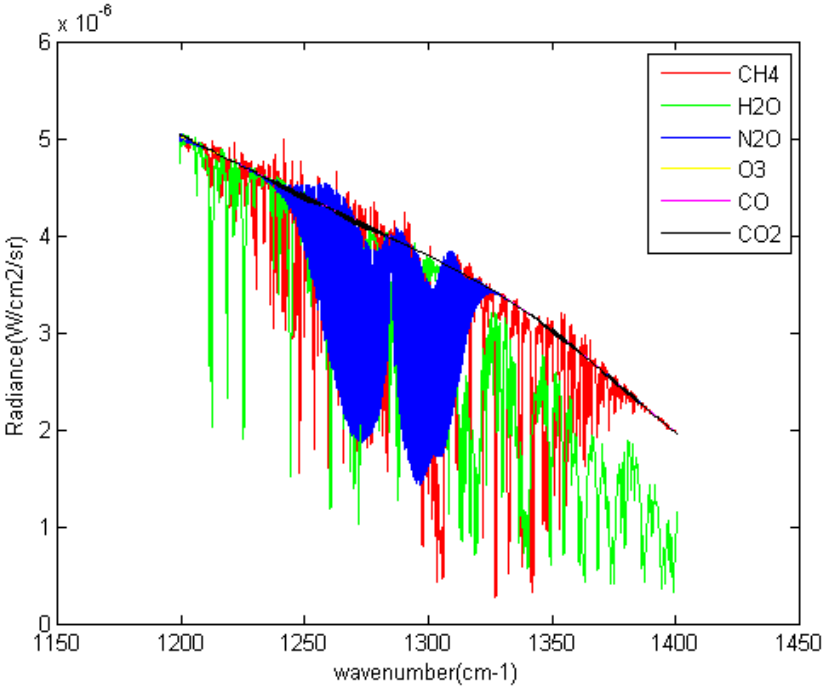

Fig. 1 Absorption of CH4, H2O, N2O, CO2, O3, and CO in the 1320–1360 cm^{-1} band.

3 Inversion Theory

3.1 Inversion Band

The main guiding principle for the selection of the inversion bands of the target gas is to obtain good sensitivity to the target gas and minimal interference with other absorptive gases. Covered by Infrared Atmospheric Sounding Interferometer (IASI) (http://smsc.cnes.fr/IASI/GPsatellite.htm; Blumsteina D et al., 2004; Masiello G et al., 2009), the infrared absorption band at 7.6 μm can be used for CH4 inversion, for which the main overlapping absorptive gases are H2O and N2O. The interference of N2O is primarily in the 1250–1320 cm^{-1} band, whereas H2O influences the whole band. As the inversion of H2O can be realized from other infrared or microwave bands, the 1320–1360 cm^{-1} band is selected to invert.

3.2 Inversion Theory

In the plane-parallel atmosphere with local thermodynamic equilibrium, at a height of z, the radiation emitted from an atmospheric layer with the depth of dz is,

$$\Delta R(z) = k(z)\rho(z)B(T(z))dz \qquad (1)$$

In equation (1), B(T(z)) is the Planck function, k(z) is the absorption coefficient of atmospheric gas composition, ρ(z) is the atmospheric gas concentration, and the contribution of the layer dz to the total radiation from the top atmosphere is

$$R = \Delta R(z)e^{-\int_z^\infty k(z')\rho(z')dz'} = B(T(Z))d\tau(z) \qquad (2)$$

In equation (2),

$$\tau(z) = e^{-\int_z^\infty k(z')\rho(z')dz'} \qquad (3)$$

is the atmospheric transmittance over the height z. Thus, the total radiation observed by the satellite detector is

$$R = \varepsilon B(T(0))\tau(0) + \int_0^{\infty} k(z)\rho(z)B(T(z))\tau(z)dz \qquad (4)$$

In equation (4), ε refers to the surface emissivity. The absorption coefficient of the atmospheric gas composition can be calculated from absorption spectrum line data sets (e.g., AFGL or HITRAN databases). Given the atmospheric temperature profile, it can be obtained the atmospheric concentration of absorptive gases using the nonlinear atmospheric radiation transfer equation expressed by equation (4). In the neighborhood of the estimated initial concentration in the atmosphere, the first-order variation to equation (4) is,

$$\delta R = \int_0^{\infty} k(\rho_0(z'))\delta\rho(z')dz' \qquad (5)$$

Equation (5) is the first kind linear Fredholm integral equation. To solve linear remote sensing equation, a series of reasonable physical inversion methods may be used, primarily including restrictive linear inversion, optimal weight function and iterative methods.

To invert the column concentration of atmospheric CH4, because the vertical distribution of CH4 is relatively homogeneous, it can be assumed that the vertical distribution of CH4 is homogeneous. Equation (5) can then be inversely solved as (Zeng Q C, 1974; Liou K N, 1991; Wallace J M and Hobbs P V, 2006)

$$\delta\rho = \frac{\delta R}{\int_0^z K(\rho_0(z'))dz'} \qquad (6)$$

4 Sensitivity Studies

For the forward modeling of thermal infrared radiation transfer in the atmosphere, the primary computing methods include the line-by-line integral method, belt model, and k-distribution method. The line-by-line integral method refers to an accurate method for computing transmittance by estimating the absorptive spectrum contribution of atmospheric gases line by line, which allows it to effectively address atmospheric radiation transfer problems of atmospheric non-uniform paths and overlapping absorption. As a result, the LBLRTM can be used to forward model thermal infrared outgoing radiation in the atmosphere.

The main features of LBLRTM are as follows (Yang Z H et al., 2002; Mao J P and Kawa S R, 2004; Ye H H et al., 2011; http://rtweb.aer.com/lblrtm.html.):

(1) The Voigt profile is used for absorption line shapes to include both collision-broadening and Doppler-broadening processes in the entire atmospheric column.

(2) The continuous absorption model MT CKD (Mlawer, Tobin, Clough, Kneizys, Davies) is employed by combining both self-broadening and outer-broadening.

(3) The HITRAN database is used as input.

(4) LBLRTM is an accurate, efficient, and well-validated line-by-line code that is broadly used in atmospheric radiation and remote sensing to validate band models. Based on comparisons of experimental and simulated simulation, the precision can reach 0.5%.

(5) It can calculate transmittance, optical depth, degree of attenuation, emittance, and

irradiance.

In the computing simulation, the U.S. standard atmosphere is employed and assuming the reference to surface emissivity to be 0.98, the boundary temperature to be 288.2 K and the spectral resolution to be 0.025 cm^{-1}.

4.1 Spectral Resolution

The spectral resolution must be improved to increase the amount of information in each observed spectrum. High signal-to-noise ratios and high spectral resolution require remote sensor manufacturing technology with higher resolution. However, the improvement of spectral resolution will double the cost of satellite and remote sensor technology. In instrument research, there is a tradeoff between improving the signal-to-noise ratio and improving the spectral resolution. Additionally, high spectral resolution also increases the issue of information redundancy, increasing the data volume and the time required to analyze the data. Therefore, the optimal selection of the resolution to obtain the largest amount of relevant information is important.

By modeling different spectral resolutions in CH_4 absorptive bands, the optimal spectral resolution is obtained to resolve the CH_4 spectral features. Fig. 2 shows the radiance obtained using three different magnitudes of spectral resolution, from 0.003 cm^{-1} to 0.25 cm^{-1}, in the 1320–1360 cm^{-1} band. Within a narrower spectrum, many absorptive valleys contain information about the CH4 concentration at different heights in the atmosphere. Comparing the spectral resolutions of 0.25 cm^{-1} and 0.003cm^{-1}, many weaker absorptive valleys cannot be distinguished at the 0.25 cm^{-1} spectral resolution. Therefore, the linear change in the absorptive line with stronger absorption and wider spectrum cannot be captured well. Comparing the spectral resolutions of 0.025 cm^{-1} and 0.003 cm^{-1}, the position of the absorptive valley or intensity essentially reflects the absorption spectrum characteristics. From a qualitative analysis viewpoint, employing a spectral resolution of 0.025cm^{-1} reflects the absorptive spectral characteristics. The following results are all obtained using this resolution and for the wave-number range of 1320–1360 cm^{-1}.

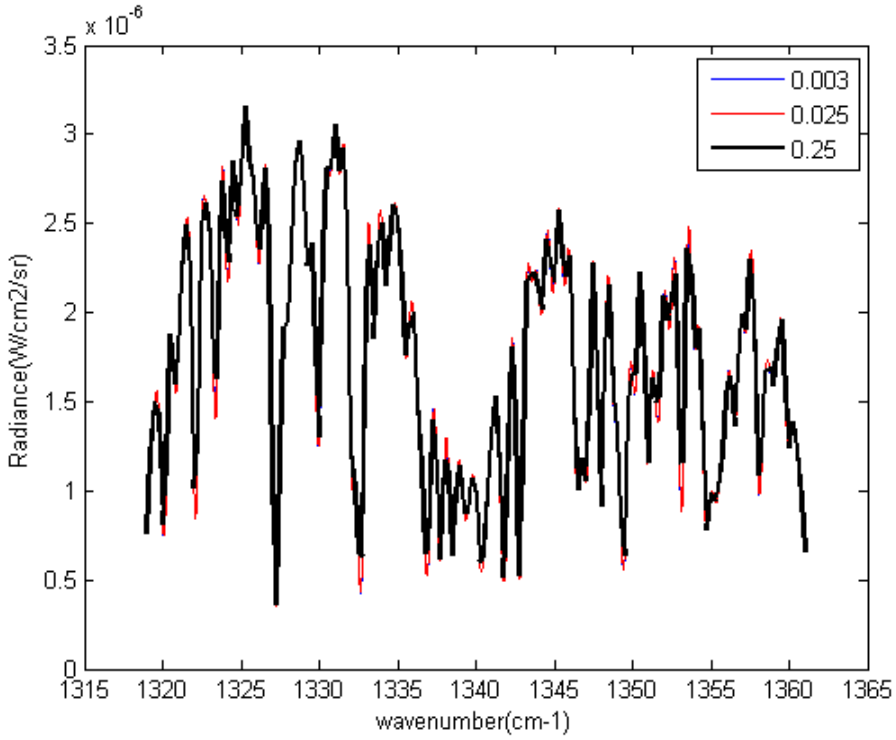

Fig. 2 Radiance obtained using three different spectral resolutions.

4.2 CH_4 Initial Profile

Because the amount of information about the target gas in this spectrum is limited, it is impossible to extract all vertical distribution information for the target gas. The large majority of the vertical distribution information for inverting the target gas depends on the initial information in the input profile, which limits the inversion result. Fig. 3 shows the change in the top atmospheric outgoing radiance: when the CH4 mixing ratio increases by 1%, the corresponding mean radiance change is 0.774%.

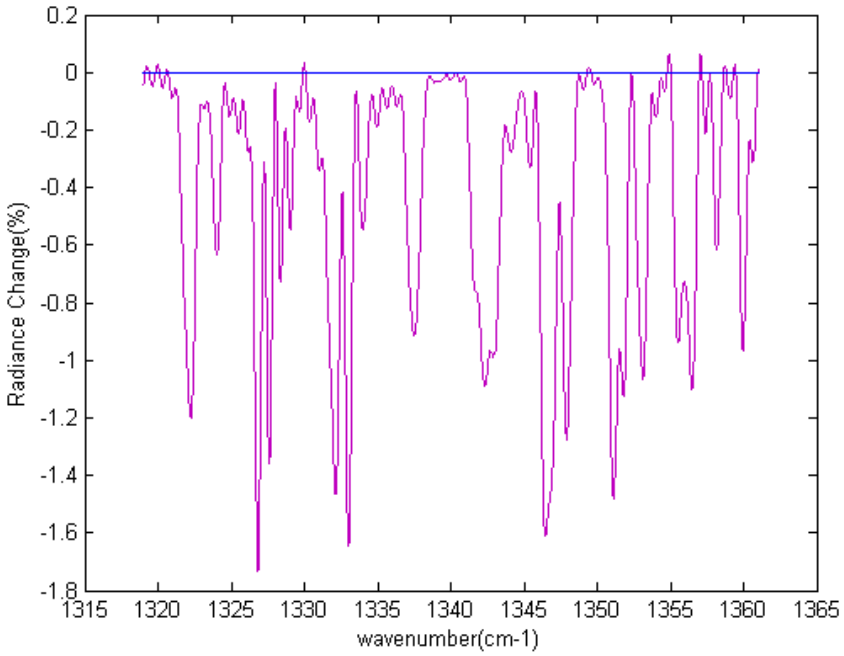

Fig. 3 Radiance change caused by a 1% increase in the CH4 content of the U.S. standard atmosphere.

To further describe the effect of the atmospheric CH4 mixing ratio at different heights on the outgoing radiance for the top of the atmosphere, Fig. 4 shows the change in the outgoing radiance in the chosen inversion band when the atmospheric CH4 mixing ratio for each layer increases by 0.1 ppmv (from an initial value of the U.S. standard atmosphere). Because the increasing CH4 concentration will reduce the atmospheric transmittance, the outgoing radiance of top atmosphere will decrease with increased CH4 concentration. However, the radiance is greater than the U.S. standard atmosphere from 20 km to 50 km, where there is significant temperature inversion. As observed in Fig. 4, the overall influence of the CH4 mixing ratio inversion error is below 0.05%, which is significantly less than the 1% CH4 change. The change in the top atmospheric outgoing radiance is less than 0.01% in the lower troposphere (0–2 km) and above 15 km (approximately the tropopause), showing that the change in the top atmospheric outgoing radiance is primarily caused by the atmospheric CH4 concentration changing from 2 km to 15 km, whereas the influence is negligible above 55 km. Moreover, the change in the top atmospheric outgoing radiance is less than 0.001% from 24 km to 32.5 km for the chemical reaction of CH4.

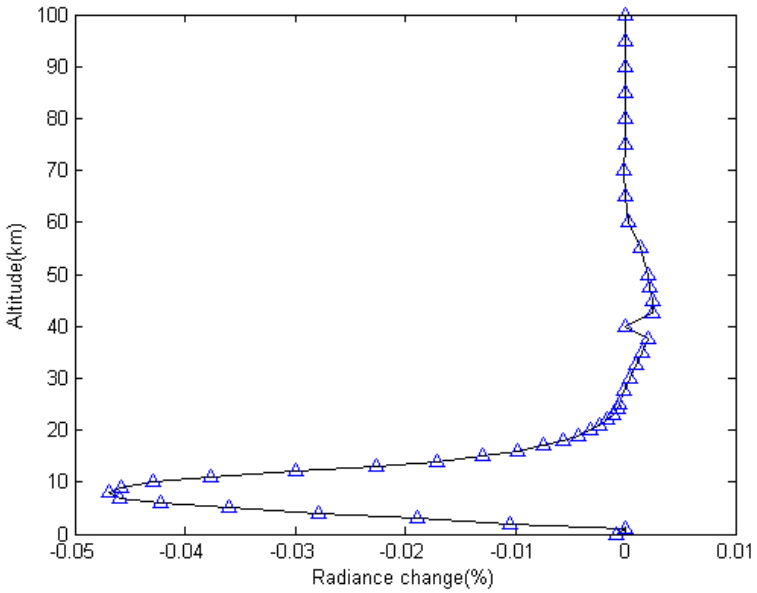

Fig. 4 Radiance change caused by the addition of a 0.1 ppmv CH4 mixing ratio to each layer of the U.S. standard atmosphere.

4.3 Temperature Dependence

The atmospheric temperature profile determines the Planck thermal radiation of each layer of the atmosphere and thus impacts the inversion precision of the atmospheric composition profile. To describe the contribution of the atmospheric temperature change to the radiance of the top atmosphere, a 1K temperature error is added to each layer of the U.S. standard atmosphere. Fig. 5 shows the radiance change after the 1K error is introduced in the temperature profile. As observed in Fig. 5, the curve shape is similar to the δ function. The overall influence of the temperature inversion error is less than the change caused by increasing the CH_4 mixing ratio by 1%. In the lower troposphere (0–2 km), the radiance sensitivity increases. The sensitivity begins to decrease from 2 km to 100 km. In detail, the change in the top atmospheric outgoing radiance is less than 0.1% over 7 km; the sensitivity is less than 0.01% over 14 km and almost constant over 60 km, indicating that the change in the top atmospheric outgoing radiance is mainly caused by the atmospheric temperature changing in the troposphere.

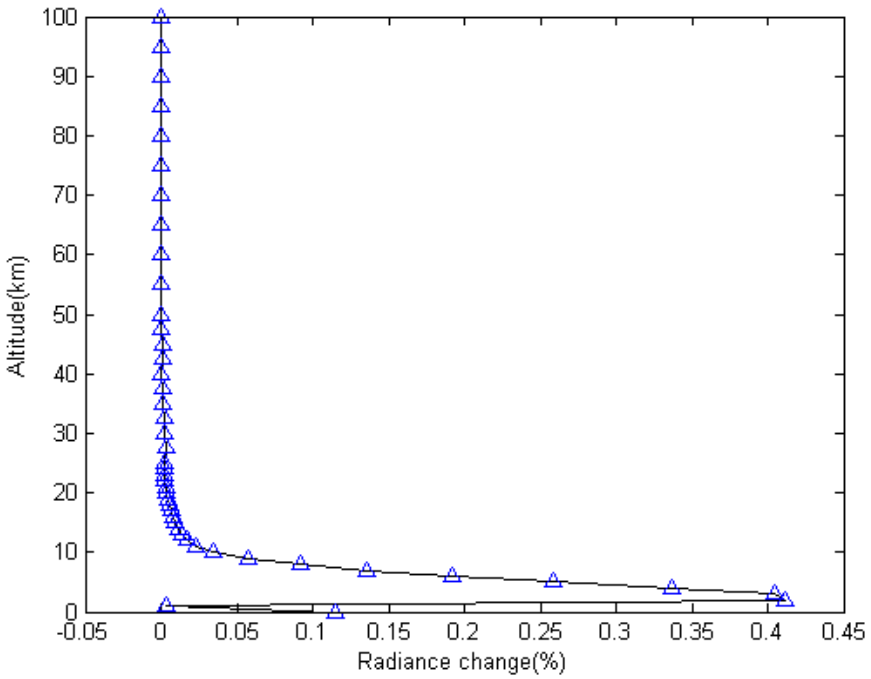

Fig. 5 Radiation change caused by a 1 K temperature increase for each layer of the U.S. standard atmosphere.

4.4 Water-Vapor Interference

Water vapor is absorbed throughout almost the entire 0–15000 cm^{-1} band which includes the near infrared solar radiation and nearly the entire infrared region (Ho S P et al., 2002). Furthermore, water-vapor has space and time variability by height in the tropospheric atmosphere. As observed in Fig. 1, water-vapor has low absorption relative to CH4 in the 1320–1360 cm^{-1} band. A 10% water-vapor increase is added to each layer of the U.S. standard atmosphere. Fig. 6 shows the radiance change after the 10% error is introduced into the water-vapor profile. The height of the peak position is 3 km, at which the sensitivity is 0.3273%, which is much smaller than that for a 1% CH_4 change. The sensitivity is less than 0.1% in the nearer ground layer and over 8 km. Knowledge of these features is highly advantageous when it is removed majority of the water-vapor influence in the column CH4 inversion. Thus, the water-vapor profile must be known with high precision to separate the contribution of the atmospheric column density variation from the signal due to changes in the atmospheric CH4 mixing ratio.

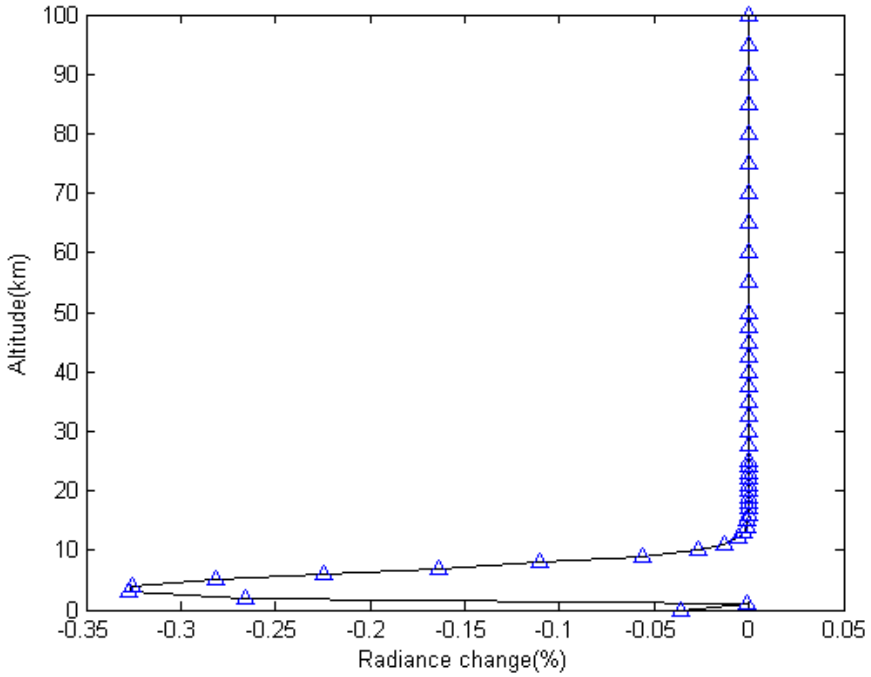

Fig. 6 Radiance change caused by a 10% increase in the water-vapor profile of the U.S. standard atmosphere.

4.5 Interference of N_2O, CO_2, O_3, CO

As shown in Fig. 1, N2O, CO2, O3, and CO have low absorption in this solar infrared band. As listed in Table 1, compared with the U.S. standard atmosphere, the influence of inversion errors of three times the N2O concentration and five times the CO2 concentration are 0.4219% and 0.4452%, respectively, which are much smaller than the change due to an increase in CH4 concentration of 1%. The interference of O3 in this band is much smaller; even the influence of 10 times the O3 concentration (0.0038%) is far less than that of a 1% increase in the CH4 mixing ratio. The radiance sensitivity is still 0, even for an increase of 10 times the CO content. Thus, CO does not absorb in this inversion band. The differences in CH4 sensitivity with and without the above mentioned greenhouse gases are negligible in our calculations for most lines. Therefore, the minor interference by the quite variable atmosphere contents of N2O, CO2, O3, and CO is a great advantage of this solar infrared band in comparison with other CH4 bands.

4.6 Surface Albedo

Surface albedo refers to the ratio of reflected radiation flux density of solar radiation on the surface to the total incident radiation flux concentration, which is also an important factor in atmospheric gas inversion. For surface albedo values of 0.01, 0.02, 0.03, 0.04, 0.05, as shown in Table 2, the larger the surface albedo, the smaller the radiance change for the top atmosphere. Furthermore, the corresponding radiance change is increasingly small when the CH4 mixing ratio increases by 1%. Additionally, the change in the CH4 content is increasingly small for the same radiation change, but the change is not obvious. However, the overall radiance change is less than that caused by an increase in the CH_4 mixing ratio by 1% of the U.S. standard atmosphere.

Table 1 Interference of N_2O, CO_2, O_3, and CO.

Concentration (ppmv)	Radiance (W cm^{-2} sr^{-1} cm)	ΔRadiance (W cm^{-2} sr^{-1} cm)	Sensitivity (%)
Standard Atmosphere	1.7215×10^{-6}	0	0
$N_2O\times2.0$	1.7178×10^{-6}	-0.3708×10^{-8}	-0.2154
$N_2O\times3.0$	1.7142×10^{-6}	-0.7264×10^{-8}	-0.4219
$N_2O\times4.0$	1.7108×10^{-6}	-1.0683×10^{-8}	-0.6206
$N_2O\times5.0$	1.7075×10^{-6}	-1.3973×10^{-8}	-0.8117
$CO_2\times2.0$	1.7195×10^{-6}	-0.1981×10^{-8}	-0.1150
$CO_2\times5.0$	1.7138×10^{-6}	-0.7665×10^{-8}	-0.4452
$CO_2\times10.0$	1.7051×10^{-6}	-1.6402×10^{-8}	-0.4452
$O_3\times2.0$	1.72147×10^{-6}	-0.7262×10^{-11}	-0.000042
$O_3\times5.0$	1.72145×10^{-6}	-2.9194×10^{-11}	-0.0017
$O_3\times10.0$	1.72141×10^{-6}	-6.5346×10^{-11}	-0.0038
CO×2.0	1.7215×10^{-6}	0	0
CO×5.0	1.7215×10^{-6}	0	0
CO×10.0	1.7215×10^{-6}	0	0

Table 2 Radiance change caused by the addition of 0.1 ppmv CH4 mixing ratio to the U.S. standard atmosphere for different surface albedo.

Albedo	Radiance (W cm^{-2} sr^{-1} cm)	ΔRadiance (W cm^{-2} sr^{-1} cm)	Sensitivity (%)
0.01	1.7219×10^{-6}	-7.8678×10^{-9}	-0.4569
0.02	1.7215×10^{-6}	-7.8626×10^{-9}	-0.4567
0.03	1.7210×10^{-6}	-7.8574×10^{-9}	-0.4565
0.04	1.7206×10^{-6}	-7.8522×10^{-9}	-0.4564
0.05	1.7201×10^{-6}	-7.8470×10^{-9}	-0.4562

From what has been discussed above, it can be seen that the interference of N2O, CO2, O3, and CO was minor in this solar infrared band overall. Minor interference from the quite variable atmospheric water-vapor content is a great merit of this solar infrared band in comparison with other CH4 solar bands, such as the 2.3 μm and 3.3 μm bands. In general, the overall radiance change result from the sensitive experiment of each factor is less than that caused by an increase in the CH_4 mixing ratio by 1% of the U.S. standard atmosphere.

5 Conclusion

Based on a 0.025 cm^{-1} spectral resolution and the use of LBLRTM as a forward model of atmospheric radiation transfer, a series of sensitivity studies have been performed to explore the influence of the CH4 initial profile, temperature, overlapping gases and surface albedo on the inversion precision of atmospheric CH_4 column density. The results indicate that a relatively small CH4 variation may be detected in the radiance measurement of reflected solar infrared radiation at 7.6 μm.

The interference of N2O, CO2, O3, and CO was minor in this solar infrared band overall. Our

full radiative transfer calculations show that the difference in CH4 sensitivity with and without water-vapor is negligible in our calculations for most layers. Therefore, minor interference from the quite variable atmospheric water-vapor content is a great merit of this solar infrared band in comparison with other CH4 solar bands, such as the 2.3 μm and 3.3 μm bands. Meanwhile, an accurate atmospheric temperature profile is required as ancillary data for the CH4 inversion. The recently launched global atmospheric temperature profilers should meet this requirement. In addition to the atmospheric temperature profile, the atmospheric column concentration is needed for analyzing the CH4 data. It can be diminished their influences on the inversion precision in the inversion real atmospheric CH_4 column concentrations only by considering the above mentioned factors and controlling their precision.

Acknowledgements

This project is supported by National Basic Research Program of China (No. 2010CB951603) and the Shanghai Science and Technology Support Program-Special for EXPO (No. 10DZ0581600). The computation was supported by the High Performance Computer Center of East China Normal University.

References

1. (1998). Kyoto Protocol to the United Nations Framework Convention on Climate Change, Kyoto, Unitied Nations
2. Khalil M A K, Rasmussen R A (1984). "Atmospheric methane: trends over the last 10000 years," *Atmospheric Enviroment*, **21**:2445-2452
3. Barrie L A, Braathen G O, Butler J H., Dlugokencky E, Hofmann D J, Tans P, Tsutsumi Y (2011). WMO Greenhouse Gas Bulletin: the State of Greenhouse Gases in the Atmosphere Using Global Observations through 2010, *WMO*, 2078-0796,
4. Forster P, Ramaswamy V, Artaxo P, Berntsen T, Betts R, Fahey D W, Haywood J, Lean J, Lowe D C, Myhre G, Nganga J, Prinn R, Raga G, Schulz M, Dorland R V (2007). Changes in Atmospheric Constituents and in Radiative Forcing, *Climate Change 2007: The Physical Science Basis, Contribution of Working Group I to the Fourth Assessment Report of the Intergovernmental Panel on Climate Change*, Solomon S, Qin D, Manning M, Chen Z, Marquis M, Averyt K B, Tignor M, Miller H L, Cambridge, United Kingdom and New York, NY, USA: Cambridge University Press, 140
5. Parker R, Boesch H, Cogan A, Fraser, Feng L, Palmer P I, Messerschmidt J, Deutscher N, Griffith D W T, Notholt J, Wennberg P O, Wunch D (2011). Methane observations from the Greenhouse Gases Observing Satellite: Comparison to ground-based TCCON data and model calculations, *Geophysical Research Letters,* **38**
6. Etheridge D, Pearma G I, Fraser P J (1992). Changes in atmospheric methane between 1841 and 1978 from a high accumulation-rate Antarctic ice core, *TellusB*,**44**:282-294
7. Grutzen P J (1995). On the role of CH4 in atmospheric chemistry: Sources, sinks and possible reductions in anthropogenic sources, *Ambio*, 24:52-55
8. Bergamaschi P, Krol M, Dentener F, Vermeulen A, Meinhardt F, Graul R, Ramonet M, Peters W, Dlugokencky E J (2005). Inverse modelling of national and European CH4 emissions using the atmospheric zoom model TM5, *Atmos. Chem. Phys.***, 5**: 2431-2460

9. Frankenberg C, Aben I, Bergamaschi P, Dlugokencky E J, Hees R V, Houweling S, Meer P, Snel R, Tol P (2011). Global column-averaged methane mixing ratios from 2003 to 2009 as derived from SCIAMACHY: Trends and variability, Journal of Geophysical Research: Atmospheres, **116**
10. Qin Y, Zhao C S (2003). *Atmospheric Chemical Basis*, Beijing, China Meteorological Press: .50-51 (in chinese)
11. Dlugokencky E J, Steele L P, Lang P M, Masarie K A(1994). The growth rate and distribution of atmospheric methane, Journal of Geophysical Research, 99: 17021-17043
12. Zhou L X, Li J L(1990). Atmospheric Environmental Chemistry, Beijing, China, Higher Education Press: 48-51, 305-306(in chinese)
13. Dai T, Shi G Y(2008). Numerical simulation study of atmospheric CO_2 concentration from FY-3 satellite, *Proceedings on Satellite remote sensing application technology and the processing method of Chinese Meteorological Society annual conference in 2008 in a breakout room* (in chinese)
14. Mao J P, Kawa S R (2004). Sensitivity Studies for spacebased measurement of atmospheric total column carbon dioxide by reflected sunlight, *Applied Optics*, **43**: 914-927
15. Ye H H, Wang X H, Wu J, Fang Y H, Xiong W, Cui F X (2011). Sensitivity for retrieval of atmospheric column carbon dioxide with high accuracy, *Journal of Atmospheric and Environmental Optics*, **6**(in chinese)
16. http://rtweb.aer.com/lblrtm.html.
17. Rothman L S, Gordon I E, Barbe A, ChrisBenner D, Bernath P F, Birk M, Boudon V, Brown L R, Campargue A, Champion J P, Chance K, Coudert L H, Danaj V, Devi V M, Fally S, Flaud J M, Gamache R R, Goldmanm A, Jacquemart D, Kleiner I, Lacome N, Lafferty W J, Mandin J Y, Massie S T, Mikhailenko S N, Miller C E, Moazzen-Ahmadi N, Naumenko O V, Nikitin A V, Orphal J, Perevalov V I, Perrin A, Cross A P, Rinsland C P, Rotger M, imecˇ kova M S, Smith M A H, Sung K, Tashkun S A, Tennyson J, Toth R A, Vandaele A C, Auwera J V(2009). The HITRAN 2008 molecular spectroscopic database, *Journal of Quantitative Spectroscopy & Radiative Transfer*, **110**
18. Shi G Y (2007). *Atmospheric Radiation*, Beijing, China, Academic Press:4-42(in chinese)
19. http://smsc.cnes.fr/IASI/GPsatellite.htm.
20. Masiello G, Serio C, Carissimo A, Grieco G, Matricardi M (2009). Application of φ-IASI to IASI: retrieval products evaluation and radiative transfer consistency, *Atmospheric Chemistry and Physics Discussions*, 9: 9647-9691
21. Blumsteina D, Chalona G, Carliera T, Buila C, Hberta Ph, Maciaszeka T, Poncea G, Phulpina T, Tournierb B, Simonic D, Astrucc P, Claussc A, Kayald G, Jegoue R(2004). IASI instrument: Technical Overview and measured performances, *roceedings of the 5th International Conference on Space Optics*, 49-56
22. Liou K N (1991). Thermal infrared Radiation Transfer in the Atmosphere, *An introduction to atmospheric radiation (Second Edition)*, California, USA, Academic Press: 116-168
23. Zeng Q C (1974). Introduction, *Atmospheric Infrared Telemetry Theory*, Beijing, China, Academic Press: 3-9(in chinese)
24. Wallace J M, Hobbs P V (2006). Radiative transfer, *Atmospheric Science, Second Edition: An Introductory Survey*, University of Washington, Academic Press: 113-121
25. Yang Z H, Toon G C, Margolis J S, Wennberg P D (2002). tmospheric CO2 retrieved from

ground-based near IR solar spectra, *Geophys. Res. Lett*, **29**:1339

26. Ho S P, Smith W L, Huang H L (2002). Retrieval of atmospheric-temperature and water-vapor profiles by use of combined satellite and ground-based infrared spectral-radiance measurements, *Applied Optics*, **41**:4057-4069

Ci SONG is a PhD candidate in Physical Geography at the Key Lab. of Geographic Information Science, East China Normal University. She received her BS in Mathematics and Applied Mathematics from Henan Normal University in 2008 and MS in Mathematics and Applied Mathematics from East China Normal University in 2011. Her research interests include differential equation and atmospheric remote sensing.

Dr. Jiong SHU is currently a professor of Climatology at the Key Lab. of Geographic Information Science, East China Normal University. He was an Honor Research Fellow at the University of Liverpool, UK, in 1999, after which he was employed as a professor at the College of Resources and Environmental Science, East China Normal University in 2000. He joined the Key Lab. of Geographical Information Science, Ministry of Education, in 2002 as the director until Dec. 2009. His research interests include climate change and environmental remote sensing.

Mandi ZHOU is a PhD candidate in Physical Geography at the Key Lab. of Geographic Information Science, East China Normal University. She received her BS and MS in Information and Computing Science from China University of Geosciences in 2006 and 2009, respectively. Her research interests include hyperspectral remote sensing and image processing.